

# Calculation of direct and indirect excitons in GaAs/Ga<sub>1-x</sub>Al<sub>x</sub>As coupled double quantum wells: The effects of in-plane magnetic fields and growth-direction electric fields

M. de Dios-Leyva,<sup>1</sup> C. A. Duque,<sup>2</sup> and L. E. Oliveira<sup>3</sup>

<sup>1</sup>*Department of Theoretical Physics, University of Havana, San Lázaro y L, Vedado 10400, Havana, Cuba*

<sup>2</sup>*Instituto de Física, Universidad de Antioquia, AA 1226 Medellín, Colombia*

<sup>3</sup>*Instituto de Física, Unicamp, Caixa Postal 6165, Campinas, São Paulo 13083-970, Brazil*

(Received 13 March 2007; revised manuscript received 21 May 2007; published 2 August 2007)

The variational procedure, in the effective-mass and parabolic-band approximations, is used in order to investigate the effects of crossed electric and magnetic fields on the exciton states in GaAs/Ga<sub>1-x</sub>Al<sub>x</sub>As coupled double quantum wells. Calculations are performed for double quantum wells under applied magnetic fields parallel to the layers and electric fields in the growth direction. The exciton envelope wave function is obtained through a variational procedure using a hydrogenic  $1s$ -like wave function and an expansion in a complete set of trigonometric functions for the electron and hole wave functions. We take into account intersubband mixing brought about by the Coulomb interaction of electron-hole pairs in double quantum wells and present a detailed analysis of the properties of direct and indirect exciton states in these systems. The present study clearly reveals anticrossing effects on the dispersion with applied voltage (or growth-direction electric field) of the photoluminescence peaks associated with direct and indirect excitons. Calculated results are found in good agreement with available experimental measurements on the photoluminescence peak position associated with direct and indirect excitons in GaAs-Ga<sub>1-x</sub>Al<sub>x</sub>As double quantum wells under growth-direction applied electric fields or under applied in-plane magnetic fields.

DOI: [10.1103/PhysRevB.76.075303](https://doi.org/10.1103/PhysRevB.76.075303)

PACS number(s): 73.20.Mf, 73.21.Fg, 71.55.Eq

## I. INTRODUCTION

A symmetric/asymmetric coupled double quantum well (DQW) consists of two identical and/or different quantum wells (QWs) separated by a thin barrier. For the symmetric case, in flatband conditions, i.e., without applied electric field in the growth direction of the heterostructure, the eigenfunctions of the DQW have well-defined symmetries which are broken in the asymmetric case. For the symmetric case and in flatband conditions, only transitions between electron and hole states with the same symmetry are optically allowed. When an electric field is applied, the electron and hole envelope wave functions are essentially localized in opposite wells and transitions that in flatband conditions were forbidden now become allowed. These kind of transitions are known as spatially indirect transitions. Whenever the maximum probability of the electron and hole wave functions is distributed in the same well, the transitions are known as spatially direct transitions. The intensity of these optical transitions is essentially given by the overlap integral of the electron and hole single-particle envelope wave functions and temperature-dependent populations of electrons and holes in the subbands. Also, it is certainly necessary to take into account the electron-hole ( $e$ - $h$ ) Coulomb interaction for an appropriate description of the optical transitions in semiconducting heterostructures. Of course, effects of the  $e$ - $h$  Coulomb interaction are essential whenever the fine structure of the optical spectra shows features which are within the range of the exciton binding energy.

Some phenomena such as exciton condensation and superfluidity have been predicted in semiconducting quantum wells<sup>1</sup> with limitations that come from the small lifetime, which is associated with the ratio between relaxation and recombination rates. This small lifetime can be increased by

some orders of magnitude when the electron and hole forming the exciton are localized in different regions of space, a situation that may be reached, for example, in DQW heterostructures under an externally applied electric field. Some studies have reported the increase of the exciton lifetime by means of a controllable variation of the exciton dispersion. It may also be reached by changes in the ground state of excitons; i.e., under perpendicularly applied electric and magnetic fields, it is possible to change the exciton ground state from a direct exciton to an indirect exciton, both in the direct space.<sup>1-4</sup> Fox *et al.*<sup>5</sup> have studied electron-sublevel-anticrossing effects in coupled QWs, mainly in the regime where the direct to indirect exciton transition occurs because, in this case, the exciton binding energy is comparable to the minimum sublevel splitting. In a study of intersubband mixing, Galbraith and Duggan<sup>6</sup> have found a blueshift in the optical transition energy in DQW systems under applied electric fields. Additionally, a minimum in the binding energy as a function of the barrier width was also attributed to the subband mixing. With the increase of the barrier width in DQWs under applied electric fields, the overlap of the electron-hole envelope wave functions strongly diminishes, which leads to an increase by 3 orders of magnitude of the exciton lifetime.<sup>7</sup> Soubusta *et al.*<sup>8</sup> have both measured and calculated the effects of an externally applied electric field on the excitonic photoluminescence (PL) in symmetric coupled DQWs. Calculations have been made using a variational procedure with good agreement between the theory and experiment for special quantities such as the electric field dependence of the excitonic binding energies, recombination energies, oscillator strengths, and relative intensities of the excitonic transitions.

By applying an in-plane magnetic field in coupled QWs, it is possible to induce strong changes in the excitonic-related

PL spectra due to field-induced displacement of the interwell exciton dispersion in momentum space, which leads to a transition from the momentum-space direct exciton ground state to the momentum-space indirect exciton ground state.<sup>9–11</sup> The indirect exciton lifetime in coupled DQW heterostructures under applied magnetic fields has been studied by Butov *et al.*<sup>9–11</sup> and they attribute the observed results to an increase in the magnetoexciton mass. Also, Butov *et al.*<sup>9–11</sup> have studied long-lifetime indirect excitons in coupled QWs and, at low temperatures and high exciton densities, strong deviations of the indirect exciton PL kinetics from monoexponential PL rise and/or decay were observed. Parlange *et al.*<sup>12,13</sup> have studied the indirect exciton dispersion in  $k$  space by considering the simultaneous effect of in-growth direction applied electric field and in-plane magnetic field in DQW heterostructures and found that the PL spectra increase with the magnetic field following a quadratic behavior. Additionally, they present measurements of the PL-peak positions of both direct and indirect excitons in biased GaAs/Ga<sub>1-x</sub>Al<sub>x</sub>As coupled DQWs under in-plane applied magnetic fields.

In the present work, we are concerned with a theoretical study of the effects of crossed growth-direction applied electric and in-plane magnetic fields on the exciton direct and indirect states in GaAs/Ga<sub>1-x</sub>Al<sub>x</sub>As coupled DQWs. The present study is organized as follows. The theoretical framework is outlined in Sec. II. Results and discussion are presented in Sec. III, and final conclusions are in Sec. IV.

## II. THEORETICAL FRAMEWORK

Here, we are concerned with the excitonic states in GaAs-Ga<sub>1-x</sub>Al<sub>x</sub>As DQWs grown along the  $z$  axis and in the presence of crossed growth-direction electric and in-plane magnetic fields. The present theoretical approach assumes the envelope-function and parabolic-band approximations.<sup>14,15</sup> We choose  $z=0$  at the barrier center, the electric field along the growth direction,  $\vec{E}=-E\hat{z}$ , and the in-plane magnetic field in the  $x$  direction,  $\vec{B}=B\hat{x}$  (see Fig. 1), and use the Landau gauge  $\vec{A}(\vec{r})=-Bz\hat{y}$ . The Hamiltonian for the exciton then takes the following form<sup>16–18</sup>

$$\hat{H} = \frac{1}{2m_e^*} \left( \hat{\vec{p}}_e + \frac{e}{c} \vec{A}_e \right)^2 + \frac{1}{2m_h^*} \left( \hat{\vec{p}}_h - \frac{e}{c} \vec{A}_h \right)^2 + V_e(z_e) + V_h(z_h) - \frac{e^2}{\epsilon|\vec{r}_e - \vec{r}_h|} + e\vec{E} \cdot (\vec{r}_e - \vec{r}_h), \quad (1)$$

where  $\vec{A}_e = \vec{A}(\vec{r}_e)$ ,  $\vec{A}_h = \vec{A}(\vec{r}_h)$ , and  $\hat{\vec{p}}_i$ ,  $\vec{r}_i$ ,  $m_i^*$ , and  $V_i$ , with  $i=e, h$ , are the momentum operators, electron and hole coordinates, effective masses, and corresponding DQW confining potentials, respectively.  $e$  is the absolute value of the electron charge and  $\epsilon$  is the GaAs dielectric constant. For simplicity, the dielectric constant and the effective masses are considered the same as in GaAs throughout the GaAs-Ga<sub>1-x</sub>Al<sub>x</sub>As DQW.

In order to find the eigenfunctions  $\Psi_{exc}(\vec{r}_e, \vec{r}_h)$  of the exciton Hamiltonian [Eq. (1)], it is important to note that the

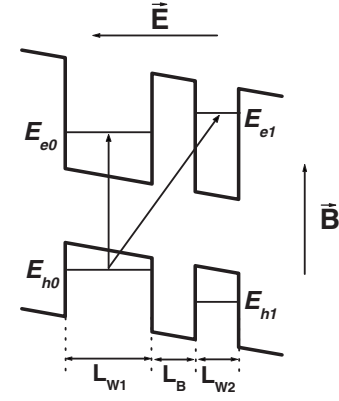


FIG. 1. Schematic view of the coupled double quantum well used in the present work. When the  $e$ - $h$  transition essentially occurs spatially at the same well, the exciton is termed as a direct or intrawell exciton, whereas the exciton is named as an indirect or interwell exciton when the corresponding  $e$ - $h$  transition occurs for the electron and hole in separated wells.

total in-plane exciton momentum  $\hat{\vec{P}} = (\hat{P}_x, \hat{P}_y)$  is an exact integral of motion<sup>16–18</sup> and the exciton envelope wave function may be written as

$$\Psi_{exc}(\vec{r}_e, \vec{r}_h) = \frac{\exp\left(\frac{i}{\hbar} \hat{\vec{P}} \cdot \vec{R}\right)}{\sqrt{S}} \Phi(\vec{\rho}, z_e, z_h), \quad (2)$$

where  $\vec{P} = (P_x, P_y)$  are the eigenvalues of the exciton momentum  $\hat{\vec{P}}$ ,  $S$  is the transverse area of the GaAs-Ga<sub>1-x</sub>Al<sub>x</sub>As DQW,  $\vec{R}$  and  $\vec{\rho}$  are the in-plane exciton center-of-mass (c.m.) and relative coordinates, respectively, and  $\Phi(\vec{\rho}, z_e, z_h)$  is the eigenfunction of the Hamiltonian

$$\hat{H} = \hat{H}_0 - \frac{e^2}{\epsilon|\vec{r}_e - \vec{r}_h|}, \quad (3)$$

corresponding to the exciton energy  $E_X$ . In the above equation,

$$\hat{H}_0 = \frac{P^2}{2M} + \frac{\hat{p}_\rho^2}{2\mu} + \hat{H}_e + \hat{H}_h, \quad (4)$$

where  $P^2 = P_x^2 + P_y^2$ ,  $\hat{p}_\rho = \hat{x}\hat{p}_x + \hat{y}\hat{p}_y = -i\hbar \frac{\partial}{\partial \rho}$ , and  $M = m_e^* + m_h^*$  and  $\mu = \frac{m_e^* m_h^*}{M}$  are the total and reduced exciton masses, respectively,

$$\hat{H}_e = \frac{\hat{p}_{ez}^2}{2m_e^*} + V_e(z_e) + \frac{1}{2} m_e^* \omega_e^2 z_e^2 - \left[ F_{eff} + \frac{eB}{m_e^* c} \hat{p}_y \right] z_e \quad (5)$$

and

$$\hat{H}_h = \frac{\hat{p}_{hz}^2}{2m_h^*} + V_h(z_h) + \frac{1}{2} m_h^* \omega_h^2 z_h^2 + \left[ F_{eff} - \frac{eB}{m_h^* c} \hat{p}_y \right] z_h. \quad (6)$$

In the last equations,  $\omega_\alpha = \frac{eB}{m_\alpha^* c}$ , with  $\alpha=e, h$ , are the cyclotron frequencies and  $F_{eff} = eE_{eff} = eE + \frac{eB}{Mc} P_y$  determines the effective electric field  $E_{eff}$ , which has the contributions of the

external electric field  $\vec{E} = -E\hat{z}$  and of the “electric field”  $\vec{E}_{c.m.} = \frac{\vec{B} \times \vec{P}}{Mc}$  that appears as a result of the direct coupling between the c.m. and the  $z$ -internal exciton coordinate. The above results indicate that from the study of the effects of  $E_{eff}$  on the exciton properties, one automatically knows the effects of both  $\vec{E}$  and  $\vec{E}_{c.m.}$  on these properties.

In order to obtain the exciton eigenfunctions for the GaAs-Ga<sub>1-x</sub>Al<sub>x</sub>As DQW under crossed electric and magnetic fields, we adopt the variational scheme used by Fox *et al.*<sup>5</sup> and Galbraith and Duggan,<sup>6</sup> which consists in minimizing the functional

$$E(\Phi) = \langle \Phi | \hat{H} | \Phi \rangle \quad (7)$$

by using the variational wave functions as

$$\Phi(\vec{\rho}, z_e, z_h) = f(z_e)F(z_h)e^{-\lambda r}, \quad (8)$$

where  $r = \sqrt{\rho^2 + (z_e - z_h)^2}$ ,  $\lambda$  is a variational parameter, and  $f(z_e)$  and  $F(z_h)$  are, in general, linear combinations of the  $z$ -dependent part of the electron  $f_i(z_e)$  and hole  $F_j(z_h)$  eigenfunctions of the total Hamiltonian neglecting the Coulomb interaction, i.e., of the  $z$ -dependent parts of the eigenfunctions of the Hamiltonians (5) and (6), respectively.<sup>4-6</sup> The coefficients  $a_i^{(e)}$  and  $b_j^{(h)}$  of these linear combinations are also variational parameters satisfying the usual normalization conditions.<sup>5,6</sup> Finally, in order to obtain the noncorrelated  $f_i(z_e)$  electron and  $F_j(z_h)$  hole eigenfunctions, it is convenient to use the method by Xia and Fan<sup>19</sup> of expansion in terms of sine functions, used in the study of electron states in semiconductor superlattices in the presence of in-plane magnetic fields. This is so that the method may be easily adapted to calculate the quasistationary states appearing in the presence of growth-direction applied electric fields when  $\mathbf{B} = 0$ . It is important to note that the presence of the momentum operator  $\hat{p}_y$  in the right-hand side of Eqs. (5) and (6) does not affect the exciton variational wave function as chosen in Eq. (8), as the eigenfunctions of  $\hat{H}_e$  and  $\hat{H}_h$  are proportional to  $e^{i\vec{k} \cdot \vec{\rho}}$  and, at low temperatures, the energy dependence on the wave vector  $\vec{k}$  may be disregarded and one may take  $\vec{k} = 0$ . Also, at low temperatures, when comparing theoretical and experimental results, one may take the exciton momentum  $\vec{P} = (P_x, P_y)$  as null. Here, we note that the assumption of the above separable exciton trial wave function introduces some limitations in the validity of calculated results. For a DQW in the presence of crossed electric and in-plane magnetic fields, confinement is a complicated competition between wave function compression provided by the magnetic field, the electric-field-induced polarization, and the DQW barrier-potential effects. By choosing a simple hydrogenlike envelope excitonic wave function, one would, therefore, expect a quantitatively realistic description of the exciton properties only in situations in which the spatial DQW barrier-potential confinement dominates and/or confinement effects due to the electric and in-plane magnetic applied fields are, at most, moderate.

In the variational approach described above, the effect of the Coulomb interaction is to mix the GaAs-Ga<sub>1-x</sub>Al<sub>x</sub>As DQW electron and hole wave functions  $f_i(z_e)$  and  $F_j(z_h)$ ,

respectively. Here, we are interested in excitons associated with the GaAs-Ga<sub>1-x</sub>Al<sub>x</sub>As DQW ground state, and limit ourselves to the cases for which only the mixing between the DQW electron ground state  $f_0(z_e)$  and electron first-excited state  $f_1(z_e)$  is important (cf. Fig. 1), whereas mixing effects for the DQW hole states are disregarded. The corresponding variational exciton wave functions (8) then take the form

$$\Phi_+(\vec{\rho}, z_e, z_h) = \Psi_+(z_e)F_0(z_h)e^{-\lambda_+ r} \quad (9)$$

and

$$\Phi_-(\vec{\rho}, z_e, z_h) = \Psi_-(z_e)F_0(z_h)e^{-\lambda_- r}, \quad (10)$$

with

$$\Psi_+(z_e) = [\alpha f_0(z_e) + \sqrt{1 - \alpha^2} f_1(z_e)] \quad (11)$$

and

$$\Psi_-(z_e) = [-\sqrt{1 - \alpha^2} f_0(z_e) + \alpha f_1(z_e)], \quad (12)$$

where  $F_0(z_h)$  is the DQW hole ground state, and  $\alpha$ ,  $\lambda_+$ , and  $\lambda_-$  are variational parameters. We follow the procedure by Fox *et al.*<sup>5</sup> in the process of minimizing  $E(\Phi)$  [cf. Eq. (7)], using the wave functions (9) and (10).

In order to compare the present theoretical results with available experimental data, it is important to know the following properties of the  $E_X(\vec{P})$  exciton dispersion. By using Eqs. (3)–(6) and the Hellmann-Feynman theorem, it is easy to show that

$$\frac{\partial E_X(\vec{P})}{\partial P_x} = \frac{P_x}{M} \quad (13)$$

and

$$\frac{\partial E_X(\vec{P})}{\partial P_y} = \frac{1}{M} \left[ P_y - \frac{eB}{c} \langle z_e - z_h \rangle \right], \quad (14)$$

where  $d = \langle z_e - z_h \rangle$  represents the mean distance of the correlated  $e$ - $h$  pair along the growth direction. It follows from Eq. (13) that the  $P_x$  dependence of  $E_X(\vec{P})$  is of the form  $P_x^2/2M$ , i.e., the externally applied electric and magnetic fields do not affect the exciton dispersion along the direction of the in-plane magnetic field. The  $P_y$  dependence of  $E_X(\vec{P})$  is not so simple, however, as, in general, it also depends on the explicit dependence of  $d$  on  $P_y$ . In the case of spatially indirect excitons, the conditions of the DQW system may be such that the correlated  $e$ - $h$  distance  $d$  is essentially independent of  $P_y$  and, therefore, Eq. (14) leads to an exciton dispersion given as

$$E_X(\vec{P}) = E_X^0 + \frac{P_x^2}{2M} + \frac{1}{2M} \left( P_y - \frac{eBd}{c} \right)^2, \quad (15)$$

where  $E_X^0$  is the exciton energy at  $\vec{P} = 0$ . For optically active indirect excitons ( $\vec{P} = 0$ ), Eq. (15) becomes

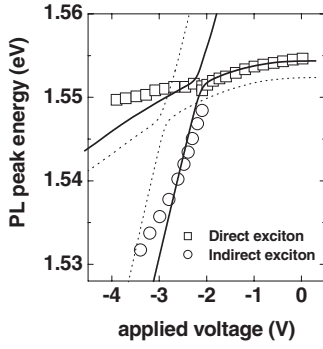


FIG. 2. PL-peak positions at  $B=0$  corresponding to direct and indirect excitons for a GaAs-Ga<sub>0.65</sub>Al<sub>0.35</sub>As DQW. Theoretical results are shown as full curves for  $L_{W1}=97$  Å,  $L_B=45$  Å, and  $L_{W2}=58$  Å, whereas experimental results associated with direct (open squares) and indirect (open circles) excitons are from Parlangelet *et al.* (Refs. 12 and 13). For comparison, calculated results for  $L_{W1}=100$  Å,  $L_B=50$  Å, and  $L_{W2}=50$  Å are also shown as dotted lines.

$$E_X(\vec{P}) = E_X^0 + \frac{e^2 B^2 d^2}{2Mc^2}. \quad (16)$$

This simple relation, in combination with PL measurements, has been used in different studies<sup>11,13,20,21</sup> of the dispersion of indirect excitons in DQWs.

### III. RESULTS AND DISCUSSION

In what follows, relevant material parameters ( $m_e^*/m_0 = 0.0665$ ,  $m_h^*/m_0 = 0.34$ , where  $m_0$  is the free electron mass, and  $\varepsilon = 12.4$ ) were taken, at low temperature, as in the work by Li.<sup>22</sup> We present, in Fig. 2, our calculated results for the PL excitonic peak positions at  $B=0$  corresponding to direct and indirect excitons in a GaAs-Ga<sub>0.65</sub>Al<sub>0.35</sub>As DQW. Theoretical results are shown for two different configurations of the DQW system:  $L_{W1}=97$  Å,  $L_B=45$  Å, and  $L_{W2}=58$  Å; and  $L_{W1}=100$  Å,  $L_B=50$  Å, and  $L_{W2}=50$  Å, and are shown in comparison with experimental measurements from Parlangelet *et al.*<sup>12,13</sup> The sample studied by Parlangelet *et al.*<sup>12,13</sup> is an asymmetric DQW made of two GaAs wells 100 and 50 Å wide, separated by a 50 Å Ga<sub>0.65</sub>Al<sub>0.35</sub>As barrier, and we noticed that the agreement with experimental data is quite good for the calculation performed with slightly different values of the widths of the GaAs wells and Ga<sub>0.65</sub>Al<sub>0.35</sub>As barrier, i.e., for  $L_{W1}=97$  Å,  $L_B=45$  Å, and  $L_{W2}=58$  Å (full curves). Also, we comment that calculated results in Fig. 2 were obtained by using a linear relationship between applied bias and corresponding electric field, and we have used a bias of  $-4$  V to correspond to a field of 70 kV/cm, as quoted by Parlangelet *et al.*<sup>12,13</sup> However, as the experimental study<sup>12,13</sup> also mentions that an applied bias of  $\sim -2$  V implies a field of  $\sim 45$  kV/cm, one should view the comparison between theoretical and experimental results in Fig. 2 with due care.

It is worthwhile to mention that two well-defined regimes are observed in Fig. 2: (i) the *direct exciton regime*, which corresponds to both the electron and hole essentially localized in the  $L_{W1}=97$  Å (or 100 Å) QW layer, and (ii) the

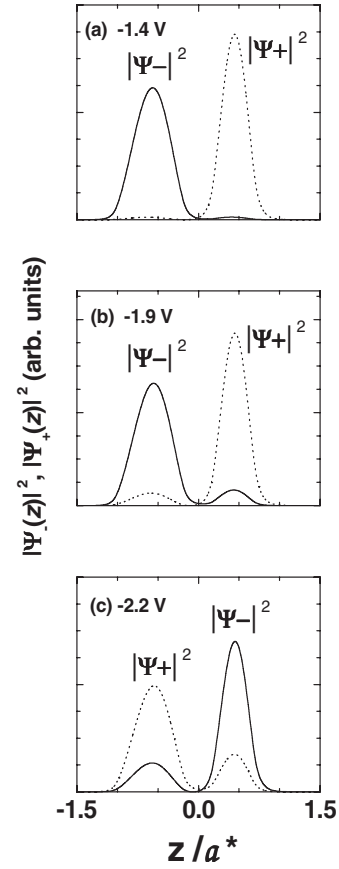


FIG. 3.  $z$ -dependent (in units of the  $a^*$  exciton effective Bohr radius)  $|\Psi_-|^2$  and  $|\Psi_+|^2$  wave functions (see text) in the case of a GaAs-Ga<sub>0.65</sub>Al<sub>0.35</sub>As DQW with  $L_{W1}=97$  Å,  $L_B=45$  Å, and  $L_{W2}=58$  Å, for different values of the applied voltage.

*indirect exciton regime*, in which case the hole wave function is localized in the  $L_{W1}=97$  Å (or 100 Å) QW layer and the electron wave function is mostly localized in the  $L_{W2}=58$  Å (or 50 Å) QW layer. Note that, for zero applied electric field, the  $\Psi_-(z_e)$  electronic wave function is mainly localized in the left well, whereas the  $\Psi_+(z_e)$  wave function is in the right well. Once the electric field is applied [cf. Eqs. (9)–(12) and Figs. 1 and 3], the hole wave function  $F_0(z_h)$  is pulled to the left of the left well, whereas the  $\Psi_-(z_e)$  electron wave function is pushed to the right well [and the  $\Psi_+(z_e)$  wave function, orthogonal to  $\Psi_-(z_e)$ , is pulled to the well at the left]. Note that the  $\Phi_-$  ( $\Phi_+$ ) exciton state [see Eqs. (9) and (10)] corresponds to the lower (higher) peak-energy curve in Fig. 2. In other words, in the absence of electric fields, the direct exciton originates essentially from the  $F_0(z_h)$  hole state combined with the  $f_0(z_e)$  electron state and corresponds to the  $\Phi_-$  exciton state [no mixing between  $f_0(z_e)$  and  $f_1(z_e)$ , cf. Eq. (12)], whereas the  $\Phi_+$  indirect exciton state is associated with the  $F_0(z_h)$  hole state combined with the  $f_1(z_e)$  electron. As the applied electric field increases, at a bias of  $\sim -2$  V, an anticrossing occurs (cf. Fig. 2) due to the strong mixture between the  $f_0(z_e)$  and  $f_1(z_e)$  wave functions [cf. Eqs. (11) and (12)], and the  $\Phi_-$  ( $\Phi_+$ ) state becomes associated with the indirect exciton (direct exciton), as clearly seen in Fig. 3. We should point out that the

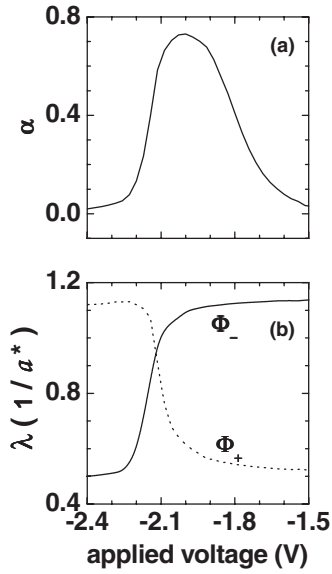


FIG. 4. Applied-voltage dependence of the  $\alpha$  and  $\lambda$  variational parameters obtained in the calculations for the  $B=0$  correlated  $e$ - $h$  transition energies for a GaAs-Ga<sub>0.65</sub>Al<sub>0.35</sub>As DQW with  $L_{W1}=97$  Å,  $L_B=45$  Å, and  $L_{W2}=58$  Å. In (b), solid (dotted) lines are for the  $\Phi_-$  ( $\Phi_+$ ) exciton state (see text), and  $a^*$  is the exciton effective Bohr radius.

experimental direct exciton PL-peak energy (cf. Fig. 2) depends only weakly on the applied voltage, whereas the corresponding theoretical line presents a much steeper dependence on the applied voltage. We believe that this is a consequence of the simple choice of a hydrogenlike variational envelope excitonic wave function together with the fact that the present theory ignores nonparabolicity and/or valence-band mixing effects.

In Fig. 4, we display the applied-voltage dependence of the  $\alpha$  and  $\lambda$  variational parameters obtained in the calculations for the  $B=0$  correlated  $e$ - $h$  transition energies for the  $L_{W1}=97$  Å,  $L_B=45$  Å, and  $L_{W2}=58$  Å GaAs-Ga<sub>0.65</sub>Al<sub>0.35</sub>As DQW, with results shown in Fig. 2. The  $\alpha$  variational parameter has the information about the contribution of each  $f_0$  and  $f_1$  electron wave function into the  $\Phi_-$  and  $\Phi_+$  excitonic wave functions [cf. Eqs. (9)–(12)]. In Fig. 4(b), the  $\lambda^+$  and  $\lambda^-$  variational parameters are shown for the two calculated exciton states, and their values indicate the spatial extension of the corresponding excitonic  $1s$ -like hydrogenic envelope wave function. For the direct exciton, as the carriers (electron and hole) are in the same QW layer,  $\lambda$  reaches its higher value (essentially the inverse of the  $a^*$  exciton effective Bohr radius, as expected) and the Coulomb interaction is quite strong, leading to a maximum in the exciton binding energy (see Fig. 5). In the case of the indirect exciton, the electron and hole originate from different wells, one has a larger spatial extension of the excitonic envelope wave function, i.e., a lower value of the hydrogenic variational parameter, leading to a weak Coulomb interaction and a lower binding energy (cf. Fig. 5). Figures 5 and 6 present the applied-voltage dependence of the exciton binding energies and excitonic PL-peak positions for the  $L_{W1}=97$  Å,  $L_B=45$  Å, and  $L_{W2}=58$  Å GaAs-Ga<sub>0.65</sub>Al<sub>0.35</sub>As DQW in the case of different

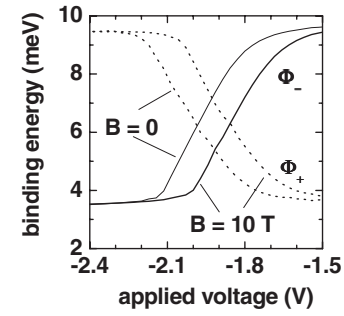


FIG. 5. Applied-voltage dependence of the exciton binding energies for a GaAs-Ga<sub>0.65</sub>Al<sub>0.35</sub>As DQW with  $L_{W1}=97$  Å,  $L_B=45$  Å, and  $L_{W2}=58$  Å, for zero field and a 10 T value of the applied in-plane magnetic field.

values of the in-plane applied magnetic field. We note that the main effect of the magnetic field is to shift the exciton anticrossing region toward higher PL-peak energy values and lower values of the applied voltage (or electric field). Of course, this could be quite easily verified in a future experimental work.

In Fig. 7, we display present theoretical results for the PL-peak energies at  $B=0$  corresponding to direct and indirect excitons for a GaAs-Ga<sub>0.67</sub>Al<sub>0.33</sub>As DQW together with

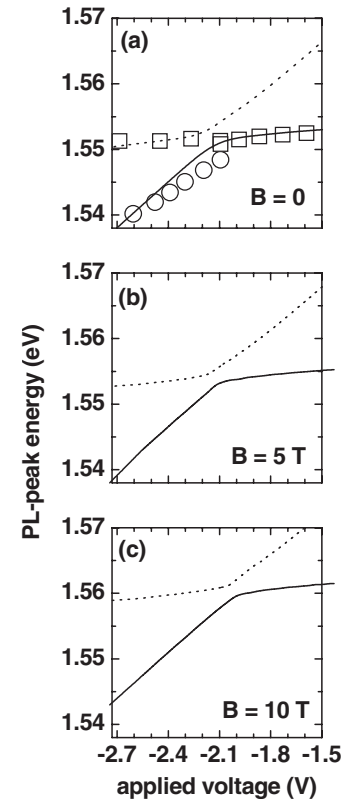


FIG. 6. Applied-voltage dependence of the PL-peak positions corresponding to direct and indirect excitons for a GaAs-Ga<sub>0.65</sub>Al<sub>0.35</sub>As DQW with  $L_{W1}=97$  Å,  $L_B=45$  Å, and  $L_{W2}=58$  Å. Results are for different values of the in-plane magnetic field: (a) zero field, (b) 5 T, and (c) 10 T. Open squares and circles in (a) are experimental results from Parlangelet *et al.* (Refs. 12 and 13).

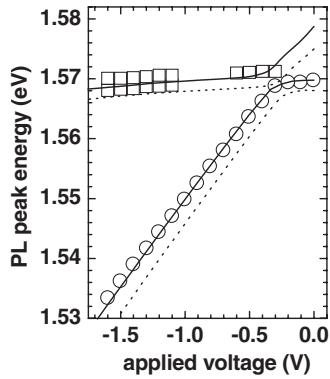


FIG. 7. PL-peak positions at  $B=0$  corresponding to direct and indirect excitons for a GaAs-Ga<sub>0.67</sub>Al<sub>0.33</sub>As DQW. Theoretical results are shown as full curves for a DQW with  $L_{W1}=78.5$  Å,  $L_B=40$  Å, and  $L_{W2}=76.5$  Å, whereas experimental results (open squares and circles) associated with direct and indirect excitons are from Butov *et al.* (Ref. 9). For comparison, calculated results for a DQW with  $L_{W1}=80$  Å,  $L_B=40$  Å, and  $L_{W2}=80$  Å are also shown as dotted lines.

the corresponding experimental measurements from Butov *et al.*<sup>9</sup> We point out that the open circles in Fig. 7 were taken from the inset in Fig. 1 of Butov *et al.*,<sup>9</sup> whereas the direct exciton PL energies shown as open squares in Fig. 7 were inferred from the  $B=0$  PL curves in Fig. 1 of Butov *et al.*<sup>9</sup> Theoretical results were obtained by using 1 kV/cm, corresponding<sup>9</sup> to 1/23.8 V. Results shown as full curves are calculations for a  $L_{W1}=78.5$  Å,  $L_B=40$  Å, and  $L_{W2}=76.5$  Å GaAs-Ga<sub>0.67</sub>Al<sub>0.33</sub>As DQW and, for comparison, we also display calculated results (dotted lines) for a  $L_{W1}=80$  Å,  $L_B=40$  Å, and  $L_{W2}=80$  Å DQW, which correspond to the nominal<sup>9</sup> widths of the GaAs-Ga<sub>0.67</sub>Al<sub>0.33</sub>As DQW sample in the experiment. Here, we note that Butov *et al.*<sup>9</sup> commented that there is a double structure in the direct exciton PL line at  $B=0$  (see open squares in Fig. 7), and point out that it is likely to result from the difference in the widths of the two QWs.<sup>23,24</sup> We believe that this would justify the fact that we have chosen the QWs with slightly different widths from the nominal value of 80 Å (theoretical results as full curves in Fig. 7). In that sense, one may view as quite good the agreement between theoretical results and experimental measurements as displayed in Fig. 7.

Finally, we depict in Fig. 8 the calculated in-plane magnetic-field dependence of the PL-peak energy in the regime of indirect exciton recombination in a GaAs-Ga<sub>0.67</sub>Al<sub>0.33</sub>As DQW and compare with experimental results from Butov *et al.*<sup>11</sup> The present theoretical results, for the whole magnetic-field range here considered, show a quadratic in-plane magnetic-field dependence of the PL peak, and agreement with experiment is only good for in-plane magnetic-field values less than  $\approx 8$  T. Of course, more theoretical work must be performed in order to adequately understand the experimental measurements by Butov *et al.*<sup>11</sup> Here, we should mention that present calculations were performed by using a simple hydrogen-like variational envelope excitonic wave function and, therefore, results should be viewed only qualitatively if confinements effects due to the in-plane

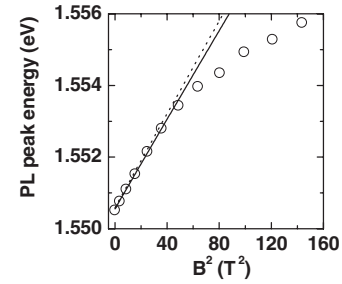


FIG. 8. In-plane magnetic-field dependence of the PL-peak position in the regime of indirect exciton recombination at applied voltage  $V_g=-1$  V for a GaAs-Ga<sub>0.67</sub>Al<sub>0.33</sub>As DQW. Experimental results from Butov *et al.* (Ref. 11) are shown as open symbols, whereas present theoretical calculations (solid line) are for  $L_{W1}=78.5$  Å,  $L_B=40$  Å, and  $L_{W2}=76.5$  Å at  $V_g=-1$  V. For comparison, calculated results for  $L_{W1}=80$  Å,  $L_B=40$  Å, and  $L_{W2}=80$  Å at  $V_g=-0.84$  V are also shown as a dotted line.

magnetic (or electric) field are comparable to or larger than the spatial QW-barrier confinement. A better quantitative description of the experimental data would certainly require a more realistic (anisotropic) description of the exciton wave function involving a combination of the appropriate solutions corresponding to the two different QW confined states and Landau levels, and by taking into account nonparabolicity and/or valence-band mixing effects. Most probably, this would, at the same time, produce a more general symmetry for the magnetoexciton states and give an appropriate agreement for the in-plane magnetic-field dependence of the PL-peak for larger values of the strength of the applied magnetic field.

#### IV. CONCLUSIONS

In conclusion, we have presented a theoretical study of the direct and indirect magnetoexciton states in GaAs/Ga<sub>1-x</sub>Al<sub>x</sub>As coupled DQWs under applied magnetic fields parallel to the layers and electric fields in the  $z$  growth direction. For calculations, we adopt the effective-mass and parabolic-band approximations and take into account inter-subband mixing brought about by the Coulomb interaction of electron-hole pairs in DQWs. The exciton envelope wave function is obtained by using a variational procedure with a hydrogenic 1s-like wave function and an expansion in a complete set of trigonometric functions for the electron and hole wave functions. Present theoretical results clearly reveal anticrossing effects on the dispersion with applied voltage (or growth-direction electric field) of the photoluminescence peaks associated with direct and indirect excitons, and are found in good agreement with available experimental measurements in GaAs/Ga<sub>1-x</sub>Al<sub>x</sub>As coupled DQWs.

#### ACKNOWLEDGMENTS

The authors are grateful to E. Reyes-Gómez for helpful suggestions in the early stages of this study. The authors would like to thank the Colombian CODI-Universidad de Antioquia and Brazilian Agencies CNPq, FAPESP, Rede

Nacional de Materiais Nanoestruturados/CNPq, and MCT-Millennium Institute for Quantum Computing/MCT for partial financial support. This work was also partially financed by the Excellence Center for Novel Materials and COLCIEN-

CIAS under Contract No. 043-2005. L.E.O. and M.d.D.L. wish to acknowledge the warm hospitality of the Departamento de Física of the Universidad de Antioquia, Medellín, Colombia, where part of this work was performed.

- 
- <sup>1</sup>Yu. E. Lozovik and V. I. Yudson, Zh. Eksp. Teor. Fiz. **71**, 738 (1976); Sov. Phys. JETP **44**, 389 (1976).
- <sup>2</sup>D. Paquet, T. M. Rice, and K. Ueda, Phys. Rev. B **32**, 5208 (1985).
- <sup>3</sup>A. Imamoglu, Phys. Rev. B **54**, R14285 (1996).
- <sup>4</sup>A. A. Gorbatshevich and I. V. Tokatly, Semicond. Sci. Technol. **13**, 288 (1998); T. Kamizato and M. Matsuura, Phys. Rev. B **40**, 8378 (1989); T. Westgaard, Q. X. Zhao, B. O. Fimland, K. Johannessen, and L. Johnsen, *ibid.* **45**, 1784 (1992).
- <sup>5</sup>A. M. Fox, D. A. B. Miller, G. Livescu, J. E. Cunningham, and W. Y. Jan, Phys. Rev. B **44**, 6231 (1991).
- <sup>6</sup>I. Galbraith and G. Duggan, Phys. Rev. B **40**, 5515 (1989).
- <sup>7</sup>A. Alexandrou, J. A. Kash, E. E. Mendez, M. Zachau, J. M. Hong, T. Fukuzawa, and Y. Hase, Phys. Rev. B **42**, 9225 (1990).
- <sup>8</sup>J. Soubusta, R. Grill, P. Hlídek, M. Zvára, L. Smrcka, S. Malzer, W. Geißelbrecht, and G. H. Döhler, Phys. Rev. B **60**, 7740 (1999).
- <sup>9</sup>L. V. Butov, A. A. Shashkin, V. T. Dolgoplov, K. L. Campman, and A. C. Gossard, Phys. Rev. B **60**, 8753 (1999).
- <sup>10</sup>L. V. Butov, A. Imamoglu, A. V. Mintsev, K. L. Campman, and A. C. Gossard, Phys. Rev. B **59**, 1625 (1999).
- <sup>11</sup>L. V. Butov, A. V. Mintsev, Yu. E. Lozovik, K. L. Campman, and A. C. Gossard, Phys. Rev. B **62**, 1548 (2000).
- <sup>12</sup>A. Parlange, P. C. M. Christianen, J. C. Maan, C. B. Soerensen, and P. E. Lindelof, Phys. Status Solidi A **178**, 45 (2000).
- <sup>13</sup>A. Parlange, P. C. M. Christianen, J. C. Maan, I. V. Tokatly, C. B. Soerensen, and P. E. Lindelof, Phys. Rev. B **62**, 15323 (2000).
- <sup>14</sup>As mentioned, here we assume the parabolic-band approximation within the effective-mass approach and note that this approximation has worked quite well in the study by Dzyubenko and Yablonskii (Ref. 15) of GaAs/In<sub>x</sub>Ga<sub>1-x</sub>As coupled QWs.
- <sup>15</sup>A. B. Dzyubenko and A. L. Yablonskii, Phys. Rev. B **53**, 16355 (1996).
- <sup>16</sup>L. P. Gorkov and I. E. Dzyaloshinskii, Sov. Phys. JETP **26**, 449 (1968).
- <sup>17</sup>K. Chang and F. M. Peeters, Phys. Rev. B **63**, 153307 (2001).
- <sup>18</sup>Y. E. Lozovik, I. V. Ovchinnikov, S. Y. Volkov, L. V. Butov, and D. S. Chemla, Phys. Rev. B **65**, 235304 (2002).
- <sup>19</sup>J.-B. Xia and W.-J. Fan, Phys. Rev. B **40**, 8508 (1989).
- <sup>20</sup>M. Orlita, R. Grill, M. Zvára, G. H. Döhler, S. Malzer, M. Byszewski, and J. Soubusta, Phys. Rev. B **70**, 075309 (2004).
- <sup>21</sup>M. Orlita, M. Byszewski, G. H. Döhler, R. Grill, S. Malzer, J. Soubusta, and M. Zvára, Physica E (Amsterdam) **30**, 1 (2005).
- <sup>22</sup>E. H. Li, Physica E (Amsterdam) **5**, 215 (2000).
- <sup>23</sup>We should point out that further studies by Butov *et al.* (Ref. 24) suggest that this double structure is associated with the direct exciton and multiparticle complexes ( $X^-$ ,  $X^+$ , etc.), with more than two particles (electrons and holes) involved in the complex.
- <sup>24</sup>L. V. Butov, A. Imamoglu, K. L. Campman, and A. C. Gossard, JETP **92**, 260 (2001).